The Use of Impedance Spectroscopy for the Characterization of Protein-Modified ISFET Devices: Application of the Method for the Analysis of Biorecognition Processes

Andrei B. Kharitonov, Julian Wasserman, Eugenii Katz, and Itamar Willner*

Institute of Chemistry, The Hebrew University of Jerusalem, Jerusalem 91904, Israel

Received: December 20, 2000; In Final Form: February 15, 2001

Impedance spectroscopy is used to characterize the structure of biomaterial layers on the gate surface of ISFET devices, and to elucidate antigen−antibody binding interactions on the gate interface. The method is based on the recording of the transfer function of the system as a function of frequency and on the extraction of the respective τ_1 and τ_2 values of the systems. From the experimental values, the film thicknesses of the respective protein layers are estimated. The method is applied to elucidate the structures of a glucose oxidase, GOx, multilayer assembly, and of a di-biotin-cross-linked avidin multilayer system. The method is also used to sense the dinitrophenyl antibody by following the formation of the antigen−antibody complex on the gate surface.

Ion-sensitive field-effect transistors (ISFETs) find growing interest in the rapidly developing field of bioelectronics.[1,2] The control of the gate potential of the ISFET device by biocatalyzed transformations that include enzymes and the respective substrates has led to the development of enzyme-based FET devices (ENFETs).[3,4] Alternatively, enzyme-labeled antigens or antibodies were employed as conjugates that control the gate potential upon antigen−antibody recognition events.[5] In most of these systems the biomaterial was encapsulated in a polymer membrane that is associated with the gate interface. In a series of recent studies[6,7] we have modified the gate surface of ISFETs with monolayers or thin films consisting of enzymes. Two general strategies were developed to control the gate interface potential: (i) the alteration of the pH of the electrolyte solution by the biocatalyzed transformation occurring at the functionalized gate surface;[6] (ii) the organization of electron-relay/enzyme monolayers that control the concentration of the relay oxidized/reduced species on the gate surface by means of the biocatalyzed reaction.[7] The advantages of the biomaterial-monolayer configurations on the ISFET devices rest on the lack of diffusion limitations for the analyzed substrate, thus leading to rapid response times of the devices. Also, while the noncovalent immobilization of biomaterials in membrane matrixes is often accompanied by the leaching of the biomaterial from the membrane, the covalent attachment of the biomaterial to the gate surface yields stable assemblies.

A major difficulty encountered in biomaterial-functionalized-ISFET devices includes the quantitative characterization of the modified gate interface. Although ingenious methods for the construction of enzyme (or protein) layers or multilayers on surfaces are available,[8,9] the quantitative assessment of surface coverage and composition is difficult. In the initial studies of monolayer enzyme-based ISFET devices[6,7] we used radioactive-labeled proteins to estimate the biomaterial surface coverage on the gate interface. This method, in addition to its inconvenience and hazard due to the use of radioactive material, is very inaccurate due to the emission scattering and absorbance by the solid support. Here we wish to introduce a novel method to characterize the biomaterial composition on the gate surface by the application of impedance spectroscopy. Developing this technique not only allows the quantitative assessment of the surface coverage of monolayer and multilayer films of proteins on the gate interface, but also provides an electronic transduction means for biorecognition events on the surface. This allows us to analyze antigen−antibody interactions on the gate of the ISFET device.

* Author to whom correspondence should be addressed. Tel: 972-2-6585272. Fax: 972-2-6527715. E-mail: willnea@vms.huji.ac.il.

Theoretical Background

Only a few reports address the impedance or capacitance features of membranes associated with ISFET devices.[10−18] These studies focus on the analysis of the capacitive and/or impedance changes of the membrane as a result of alterations in its chemical composition,[10−12] or formation of bioaffinity complexes, such as antigen−antibody complexes in the membrane.[14−18] The impedance of the membrane associated with the ISFET can be represented[10,19] by the equivalent circuit shown in Figure 1A. It consists of the input element of the ISFET device that is composed of the silicon-electrode resistance, R_{Si}, the space-charge capacitance, C_{sc}, and the oxide-insulator capacitance, C_{ox}, that is linked in series to the second element corresponding to the membrane, connected in series to the third element corresponding to the electrolyte solution resistance, R_{sol}. The membrane element of the equivalent circuit is divided into two parts that are linked in series: one part includes the bulk membrane properties, i.e., the bulk capacitance of the membrane, C_{mem}, in parallel with the bulk membrane resistance, R_{mem}. The second part includes the interfacial properties of the membrane and is composed of the double-layer capacitance at the membrane interface, C_{dl}, in parallel with charge-transfer resistance at the membrane interface, R_{ct}, and the input of the Warburg impedance, W, originating from the diffusion of ions to the membrane interface. This equivalent circuit can be simplified and depicted in the configuration shown in Figure 1B. When the semiconductor operates in the inversion regime, C_{sc} is significantly smaller than C_{ox} and may be neglected. Also, the silicon-electrode resistance, and the solution

10.1021/jp0045383 CCC: $20.00
Published on Web 04/20/2001

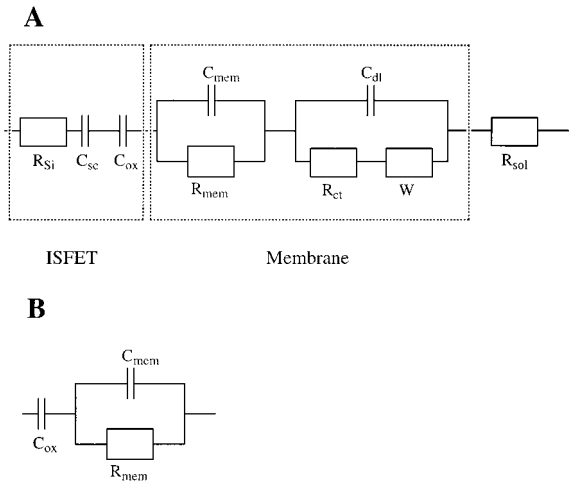

Figure 1. (A) Equivalent circuit of an ISFET device modified by a membrane film on the gate interface. (B) Simplified equivalent circuit corresponding to a membrane-functionalized ISFET device.

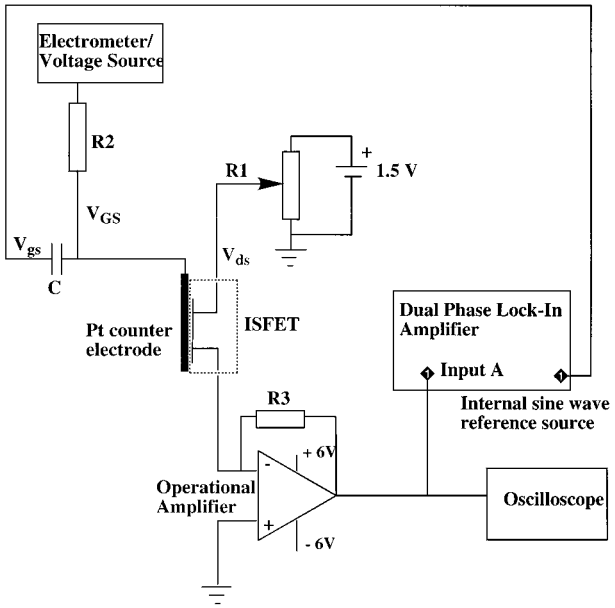

Figure 2. Electronic circuit for the determination of the transconductance of the film-modified ISFET device.

resistance are substantially lower than the membrane resistance, R_{mem}. The interfacial features of the membrane have an important contribution to the circuit at low frequencies (≤5 Hz).[20] However, at high frequencies (≥5 Hz), the interfacial properties of the membrane have no important contribution to the impedance features of the system, leading to the simple equivalent circuit where the C_{ox} unit is in series with an element consisting of the C_{mem} and R_{mem} in parallel, Figure 1B. A relaxation time of the membrane, τ, can be experimentally deduced by the electronic circuit, with the incorporated ISFET/counter-electrode, depicted in Figure 2. The voltage applied between the counter-electrode and the source of the ISFET device, V_{GS}, leads to a source-drain current, I_D. The application of the small sinusoidal voltage variations on the counter-electrode, δV_{GS}, leads to small drain-current variations, δI_d. The transconductance, $g_m = \delta I_d/\delta V_{GS}$, is then frequency-dependent.[21] The output voltage, V_{out}, is related to I_D, g_m as given by eq 1, where R represents electrical resistance in

$$V_{out} = -RI_d = -Rg_m \cdot V_{GS} \tag{1}$$

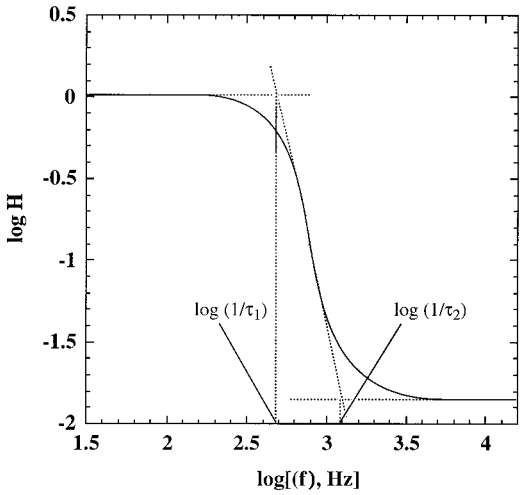

Figure 3. Theoretical transfer function and extrapolation methods to extract the τ_1 and τ_2 values.

the measuring circuit. When a membrane is associated with the oxide gate layer, the applied potential V_{GS} is divided over the membrane and the oxide layers. Thus, the effective potential difference between the gate and source is smaller than the applied value V_{GS}. A frequency-dependent transfer function, $H(j\omega)$, defined by eq 2,

$$H(j\omega) = \frac{1 + j\omega\, R_{mem}C_{mem}}{1 + j\omega\, R_{mem}(C_{mem} + C_{cox})} \tag{2}$$

is introduced to relate to the applied voltage and to the output voltage, eq 3.

$$V_{out} = Rg_m H(j\omega)\, V_{GS} \tag{3}$$

The frequency-dependent transfer function is defined by the elements of the simplified equivalent circuit, Figure 1B. The theoretical dependence[10,21] of the transfer function at variable frequencies is depicted in Figure 3. The method to extract the time constants τ_1, eq 4, and τ_2, eq 5, is shown in Figure 3. The

$$\tau_1 = R_{mem}(C_{mem} + C_{ox}) \approx R_{mem}C_{ox} \tag{4}$$

$$\tau_2 = R_{mem}C_{mem} \tag{5}$$

intersection of the two linear segments at low frequency yields the τ_1 value. Since at low frequencies the oxide layer capacitance is substantially higher than the adhered membrane, the term C_{mem} can be neglected, eq 4. In contrast, at high frequencies, the impedance values of the membrane bulk resistance (R_{mem}) and the capacitance of the membrane (C_{mem}) tend to dominate the contribution from the oxide capacitance (C_{ox}), and therefore the latter can be neglected,[22] eq 5. The τ_2 value is extracted from the intersection of the two linear segments at high frequencies. By the determination of τ_2 and the value of R_{mem} from the independent C_{ox} measurement the membrane capacitance C_{mem} can be elucidated. The membrane capacitance is given by eq 6,

$$C_{mem} = \frac{\epsilon_o \epsilon_{mem} A}{\delta_{mem}} \tag{6}$$

where $\epsilon_o = 8.85 \times 10^{-12}$ F m^{-1} is the dielectric constant of the vacuum, ϵ_{mem} is the relative dielectric constant of the attached film on the gate surface, A is the geometric area of the layer,

and δ_{mem} is the film thickness. In the present study, we immobilize protein layers or multilayers on the oxide gate surface by the covalent attachment of the biomaterials on a preassembled aminopropylsiloxane film on the gate surface. The aim of the study is to develop a method to estimate the protein layer/multilayer thickness on the gate surface, and to derive from the resulting value estimated surface coverages. Similarly, measurement of thickness variations on the gate surface upon binding of a protein could act as a method to probe bioaffinity interaction that proceeds on the gate interface. To use this method to estimate the thickness of the protein layer(s), the dielectric constant of the base siloxane should be almost unaltered upon the build-up of the biomaterial layers. This condition will be met provided the aminosiloxane layer is thick compared to the protein layer(s). The method is, however, valid to determine the siloxane film thickness, and thus prior to the assembly of the proteins on the interface, the thickness of the base layer must be determined.

Experimental Section

Chemicals and Reagents. Glucose oxidase, GOx, (E. C. 1.1.3.4) type X-S from *Aspergillus niger*, biotin, avidin, *N*-2,4-dinitrophenyl-ϵ-amino-*n*-caproic acid (DNP-antigen) and 2,4-dinitrophenyl antibody (DNP-Ab) were purchased from Sigma and used as supplied. Biotinyl−hexaethyleneglycol dimer (PEO−biotin dimer, di−biotin) from Pierce, glutaric dialdehyde (50% w/w aqueous solution), (3-aminopropyl)triethoxysilane, and other materials from Aldrich were used as supplied. Ultrapure water from ELGASTAT (UHQ) source was used in all the experiments. An aqueous solution of sodium chloride of low ionic strength, 0.01 M, was used as a background electrolyte solution in all the measurements.

Modification of the ISFET Devices. The primary modification of the Al_2O_3 gate of the ISFET was performed by dipping the gate in a 1.5 mL solution of (3-aminopropyl)triethoxysilane (10% v/v solution in toluene) that includes 100 μL H_2O for 2−3 h. The silylated chips were thoroughly rinsed with toluene and distilled water, and dried in air at room temperature for 3 h. To attach the first layer of GOx, the amino-functionalized ISFETs were first activated with glutaric dialdehyde by dipping the chip in an aqueous solution consisting of 10% (w/w) glutaric dialdehyde and 0.05 M phosphate buffer solution, pH = 7.2. The ISFETs were dried in air for 20 min and immersed in a solution of GOx (2 mg mL^{-1} in 0.05 M phosphate buffer solution, pH = 7.2) for 2 h. The modified ENFETs were rinsed with 0.05 M phosphate buffer solution and dried in air for 2 h. To construct the GOx multilayers on the gate, the two steps that include glutaric dialdehyde functionalization followed by treatment with GOx were repeated consecutively to generate the desired number of layers.[23]

To study the layered avidin−biotin systems, the amino-functionalized ISFETs were first immersed in a solution of biotin (2 mg mL^{-1} in 0.01 M HEPES-buffer solution, pH = 7.2) containing EDC (10 mM) for 2 h. The resulting devices were thoroughly rinsed with HEPES-buffer solution. Then the biotin-modified ISFETs were immersed in a solution of avidin (1 mg mL^{-1} in 0.05 M phosphate buffer solution, pH = 7.2) for 1 h and thoroughly washed with the phosphate buffer. A controlled number of avidin layers on the ISFET device was assembled by the stepwise interaction of the base avidin layer with a di-biotin solution (2 mg mL^{-1}, 0.05 M phosphate buffer solution, pH = 7.2) followed by the reaction with avidin (1 mg mL^{-1}, 0.05 M phosphate buffer solution, pH = 7.2).

The ISFETs modified with the DNP-antigen were prepared by treating the aminosiloxane-functionalized ISFETs with a solution consisting of 100 μL of ethanol and 1 mL HEPES-buffer solution (0.01 M, pH = 7.2) that included 0.5 mg of *N*-2,4-dinitrophenyl-ϵ-amino-*n*-caproic acid and EDC, 1 mg, for 2 h. The resulting DNP-antigen-modified devices were rinsed with ethanol and HEPES-buffer.

All electrodes were subjected to the impedance analyses immediately after preparation.

Measurement Procedures. The functionalized field-effect transistors (IMT, Neuchâtel, Switzerland) with an Al_2O_3 gate (20×700 μm), and a Pt wire ($d = 0.8$ mm) acting as a counter electrode and positioned 2 mm from the ISFET gate were mounted in a cell that includes 0.8 mL of the electrolyte solution. The ISFET characteristic curves (I_d vs V_{ds} for the appropriate V_{gs} values) were recorded using an HP 4155B semiconductor parameter analyzer. The measurement setup consisted of a programmable electrometer (Keithley 617), a lock-in amplifier (Stanford Research System, Model SR 830 DSP), and a two-channel digital real-time oscilloscope (Tektronix TDS 220). For impedance spectroscopy measurements on the ISFET devices, the ISFET was conjugated to the electronic circuit outlined in Figure 2 depicting the schematic diagram for the transconductance measurements. In these measurements the drain-source voltage, V_{ds}, was adjusted to 1.5 V as indicated on a SKL MAS830L multimeter using the potentiometer R1. Then the Keithley voltage source was adjusted to provide a DC bias of 750 mV and an I_d of 100 μA was passed through the device using the same multimeter. These ISFET operating conditions gave an undistorted operational amplifier (OP) output, detected on the Tektronix oscilloscope, when an AC voltage (V_{gs}) of 300 mV RMS was applied from the internal sine wave reference of the lock-in amplifier. The OP resistor R3 (820 Ohm) was chosen to provide a suitable input to the lock-in amplifier. Resistor R2 (10 kOhm) prevents an overload current in the Keithley electrometer from occurring and the capacitor (C) of 100 μF decouples the DC bias from the reference source over the frequency range cited below.

To determine the transconductance transfer functions, the output potential, V_{out}, at variable frequences (from 1 Hz to 100 kHz) were related to the modulus of impedance, Z, the real impedance, Z_{re}, and the imaginary impedance, Z_{im} ($Z = \sqrt{Z_{re}^2+Z_{im}^2}$). The values of the output potentials corresponding to Z, Z_{re}, and Z_{im} were normalized to the respective values at 1 Hz to give the respective transfer functions H. For example, the imaginary impedance transfer function is given by eq 7. When excited directly by the biased reference source from the lock-in amplifier, the operational amplifier was found to be flat within 1% over the entire frequency range.

$$\log |H| = \frac{V_{out_{im}}(f\ \mathrm{Hz})}{V_{out_{im}}(1\ \mathrm{Hz})} \tag{7}$$

The molecular dimensions of the respective proteins were estimated using commercial software HyperChem (Release 2) for Windows. The protein structures were taken from the Protein Data Bank (Brookhaven National Laboratory).[24] The errors in the calculated dimensions of the proteins is estimated to be ±5 Å.

Results and Discussion

Scheme 1 depicts the method to assemble multilayers of the enzyme glucose oxidase, GOx, on the gate of the ISFET device. The Al_2O_3 gate surface was modified with (3-aminopropyl)-triethoxysilane to yield the amino-functionalized surface. This

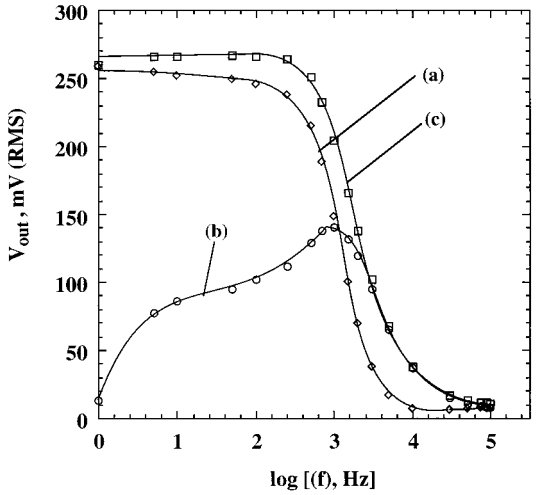

Figure 4. Output potentials of the film-modified ISFET device at variable frequencies corresponding to the different transconductance functions: (a) Modulus of impedance, *Z*. (b) The real impedance, Z_{re}. (c) The imaginary impedance, Z_{im}. All of the measurements were performed on the aminopropylsiloxane-functionalized ISFET.

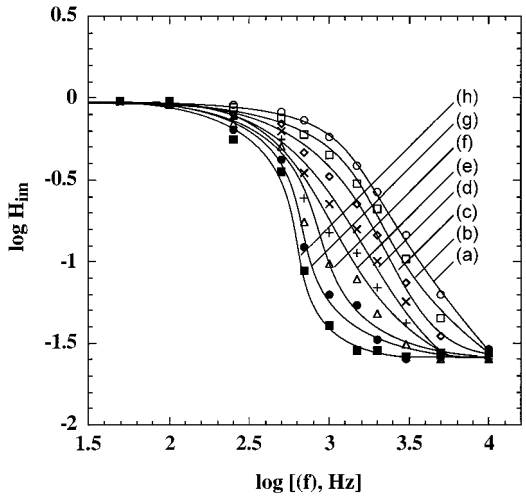

Figure 5. Transconductance, H_{im}, curves at variable frequencies for (a) the aminopropylsiloxane-functionalized ISFET; (b) to (h) the deposition of one to seven layers of glucose oxidase.

was then treated with glutaric dialdehyde and subsequently with GOx to yield the first protein layer on the gate surface. By repeated stepwise treatment of the interface with glutaric dialdehyde and then GOx, a controlled and programmed number of enzyme layers were assembled on the gate surface. Figure 4 shows the output potential at variable frequencies (from 1 Hz to 100 kHz), of the system functionalized by the aminopropylsiloxane layer assembled on the gate, related to the modulus of impedance, *Z*, curve (a), the real impedance, Z_{re}, curve (b), and the imaginary impedance, Z_{im}, curve (c). The real impedance, Z_{re}, curve (b), shows a complex peak-shaped frequency dependence that does not shift upon variation of the modified layer. Thus, this component of the impedance is not relevant to our analytical aim. The frequency-dependent output voltages of the modulus impedance *Z* and Z_{im} are almost similar and exhibit the shape of the theoretical transfer function of ISFETs. The Z_{im} curve is shifted toward higher frequencies, where impedance measurements are favored due to diminished conductive contributions of surface states and better isolation of capacitive effects. Thus, the frequency-dependent voltage output, $V_{out_{im}}$, corresponding to Z_{im} is used throughout this study to define the transfer functions at variable frequencies for the different systems (see Experimental Section, eq 7) and is denoted as V_{out}.

Figure 5 shows the transconductance at variable frequencies for the ISFET system that includes aminopropylsiloxane base film on the gate, curve (a), and for the systems that include one to seven GOx layers. From the transconductance curve, corresponding to the aminosiloxane layer, taking into account the respective dielectric constant of the film $\epsilon = 4.5$, and using eqs 4−6, we estimate the thickness of the aminosiloxane film

SCHEME 1: Stepwise Assembly of the Glucose Oxidase, GOx, Multilayer Structure on the Gate Interface of the ISFET

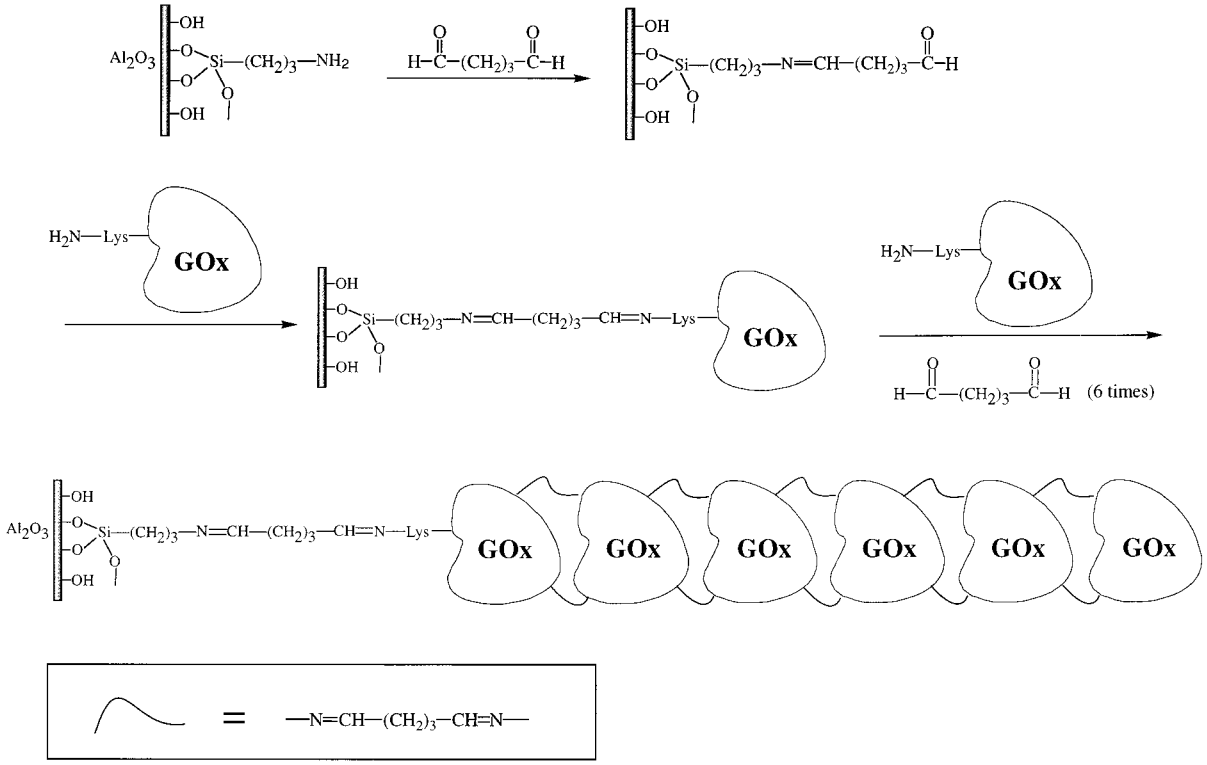

to be 500−800 Å. It should be noted that the immobilized aminosiloxane film was assembled on the gate surface under conditions that yield a relatively thick film rather than a monolayer. This structure of the aminosiloxane film was predesigned in order to retain almost constant the dielectric constant of the membrane upon the build-up of the protein layers. The thickness values of the aminosiloxane films are substantially larger than the characteristic diameter of proteins 50−150 Å and hence the dielectric constant of the film associated with the gate is almost unaltered upon the build-up of the protein layers, a prerequisite to determine the protein layer thicknesses. Also, since the dielectric constants of aminopropyl siloxane and the enzymes used are close (refractive index $n = 1.43$ and 1.45, respectively), we assume that the overall dielectric constant of the system is constant. It should be noted that the experimental procedure to assemble the aminosiloxane film was optimized to yield the appropriate film thickness, and in order to adopt the method for measuring the linked film thicknesses, this protocol should be followed precisely. Figure 5, curves (b) to (h), shows the frequency-dependent transconductance curves observed for different numbers of GOx layers assembled on the gate interface. The assembly of the GOx layers on the aminosiloxane film results in a nonsymmetrical shift of the transconductance curve to lower frequencies. For the first GOx layer, curve (b), this results in an increase in the relaxation time τ_2 from 0.002 to 0.05 ms, and a smaller change in the τ_1 value from 1.00 to 1.12 ms. The increase in τ_2 upon the build-up of the first GOx layer must be attributed to a change in the membrane capacity, C_{mem}, associated with the gate, eq 5. Although we were unable to trace the precise value of the dielectric constants of the proteins used in the present study, we estimate the dielectric constant of the protein to be ca. 3−4. Thus, taking into account the aminosiloxane film thickness, we assume that the assembly of the GOx layer practically does not influence the dielectric constant of the membrane. This implies that the observed change in τ_2 and the membrane capacity upon the build-up of the first GOx layer, originates from the change in the membrane thickness, δ_{mem}, as a result of the association of the protein layer. From Figure 5, curve (b), we estimate the thickness of the first GOx layer to be 30 ± 5 Å.

The changes in the value of τ_1, albeit small, are more difficult to explain. As at low frequencies the membrane capacity can be neglected, τ_1 is a function of the oxide layer capacity, C_{ox}, and the membrane resistance, R_{mem}. The oxide layer capacitance, C_{ox}, is, however, constant and independent of the associated films. Similarly, the membrane resistance, R_{mem}, is weakly influenced by the membrane thickness, and thus very small change in τ_1 should be detected. The observed small but significant shift in the relaxation-time, τ_1, can thus be attributed to changes in the membrane capacity, C_{mem}, as a result of the assembly of the aminosiloxane/GOx film on the oxide layer of the gate interface (cf. eq. 4).

From the different transconductance curves corresponding to the different number of GOx layers assembled on the gate surface, the thickness of the protein assembly consisting of variable layers was determined. Figure 6 shows the changes in the protein film thickness upon the assembly of GOx layers. While the thickness of the first GOx layer is ca. 30 ± 5 Å, from the second layer the thickness increases almost linearly with an average thickness increase of ca. 45 ± 5 Å per layer. The slightly lower thickness of the first GOx layer may be attributed to the porous, rough, base aminosiloxane film. Modification of the pores does not add to the film thickness, leading to the lower experimental film thickness. Glucose

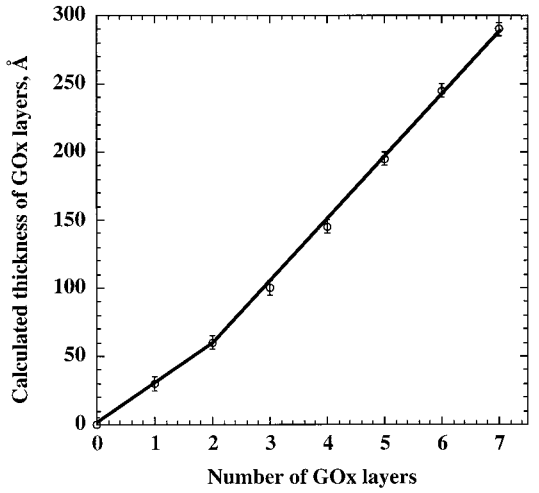

Figure 6. Calculated film thickness of GOx multilayers assembled on the aminopropylsiloxane interface associated with the ISFET.

oxidase has an average diameter of ca. 67 ± 5 Å, estimated by the use of HyperChem for Windows software and the Protein Data Bank, Brookhaven National Laboratory.[24] Thus, a densely packed monolayer of GOx exhibits a surface coverage of ca. 2.8×10^{-12} mol cm^{-2}. The experimental average thickness of GOx layers 2 to 7 is ca. 45 ± 5 Å that corresponds to ca. 65% of a densely packed monolayer. Thus, we conclude that the surface coverage of GOx per layer is ca. 1.8×10^{-12} mol cm^{-2}.

To further support the approach of using impedance spectroscopy for the characterization of layered assemblies of proteins on ISFET devices, we characterized the layered system composed of avidin−biotin. Scheme 2 outlines the method that was employed to construct the biotin−avidin layered structure on the Al_2O_3 gate of the ISFET. Biotin (**1**) was covalently coupled to the base aminopropylsiloxane layer. Avidin that has a very high association constant with biotin,[25] $K_a = 10^{15}$ M^{-1}, was then linked to the biotin units to yield the first protein layer. By the stepwise reaction of the system with the di-biotin, (**2**), followed by the interaction of the system with avidin, a controlled number of avidin layers was linked to the gate interface. Note that avidin includes four binding sites for biotin, a feature that enables the construction of the layered structure shown in Scheme 2. As the dimensions of avidin are substantially higher than those of the cross-linking biotin or di-biotin units, the contribution to the layer's thickness mainly originates from the protein component.

Figure 7 shows the frequency-dependent transconductance curves of the aminopropylsiloxane film assembled on the Al_2O_3 oxide gate, curve (a), followed by the transconductance curves of one to six avidin layers assembled on the siloxane film, curves (b) to (g). As before, the assembly of the biotin−avidin layers on the aminosiloxane film results in a nonsymmetrical shift to lower frequencies of the transconductance curves. For the first avidin layer, curve (b), the relaxation time τ_2 increases from 0.006 to 0.09 ms, whereas the τ_1 value changes from 1.02 to 1.10 ms. Using eqs 5 and 6 we estimated the thickness of the protein film that includes variable numbers of avidin layers. Figure 8 shows the calculated thickness of the avidin film that includes a various number of layers. The first avidin layer reveals a thickness that corresponds to 30 ± 5 Å, while layers two to six reveal an average thickness of 80 ± 10 Å. Although the dimensions of avidin, diameter 62 ± 5 Å, are very similar to the dimension of GOx 67 ± 5 Å, we find that the average thickness of the avidin layer is substantially higher than that of GOx. To account for this difference, we refer to the fact that

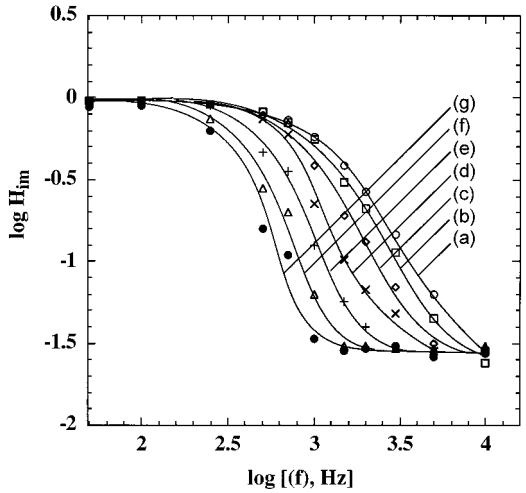

Figure 7. Transconductance, H_{im}, curves at variable frequencies corresponding to (a) the aminopropylsiloxane-modified gate interface; (b) to (g) the assembly of one to six avidin layers cross-linked by di-biotin (**2**).

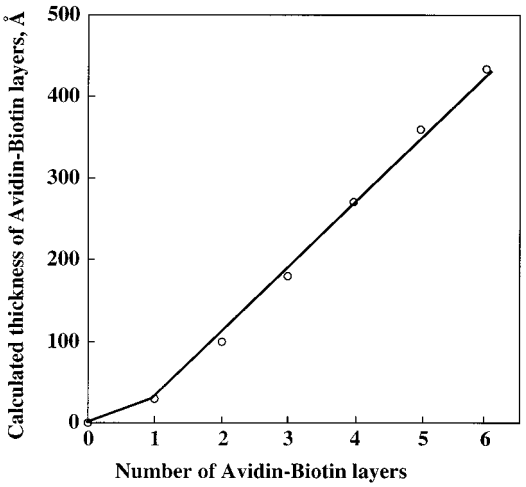

Figure 8. Calculated film thickness of avidin multilayers cross-linked by di-biotin, (**2**).

avidin has four binding sites for biotin. This enables the two-dimension intralayer cross-linking of the second to sixth avidin layers by the di-biotin units. This process allows the filling of any pinholes in the avidin layers and the formation of almost ideal densely packed monolayers of avidin on the gate surface. The first avidin layer assembled on the aminopropylsiloxane layer reveals, however, a surface coverage of only ca. 40% of the densely packed configurations observed for layers two−six. This lower thickness of the first avidin layer may be attributed to two reasons. (i) The first layer includes the association of avidin to a biotin monomer. This eliminates the two-dimensional cross-linking of the avidin units, and the formation of a densely packed monolayer. The first avidin layer could have, at best, a thickness of a random dense monolayer (corresponding to 60% of a dense monolayer configuration). (ii) Parts of the first avidin layer may be incorporated in pores of the aminosiloxane film. The diameter of avidin is 62 ± 5 Å (Protein Data Bank, Brookhaven National Laboratory).[24] We find that the average thickness of the avidin layer is slightly higher, 80 ± 10 Å. This may be attributed to the contribution from the di-biotin cross-linking units to the film thickness and to the eventual contribution of the protein dielectric constant to the dielectric constant of the resulting membrane. Note that an increase in the dielectric constant of the membrane would lead to a higher value of the membrane thickness.

The ability to characterize, by the transconductance measurements, the thickness changes of protein layers associated to the aminosiloxane film linked to oxide layer of the gate interface, suggests that one may utilize the method for the transduction of biorecognition events that occur on the gate interface. Toward this goal we were interested in applying the transconductance measurements to probe antigen−antibody affinity interactions,

SCHEME 2: Stepwise Assembly of the Crosslinked Avidin Multilayer Structure on the ISFET Device

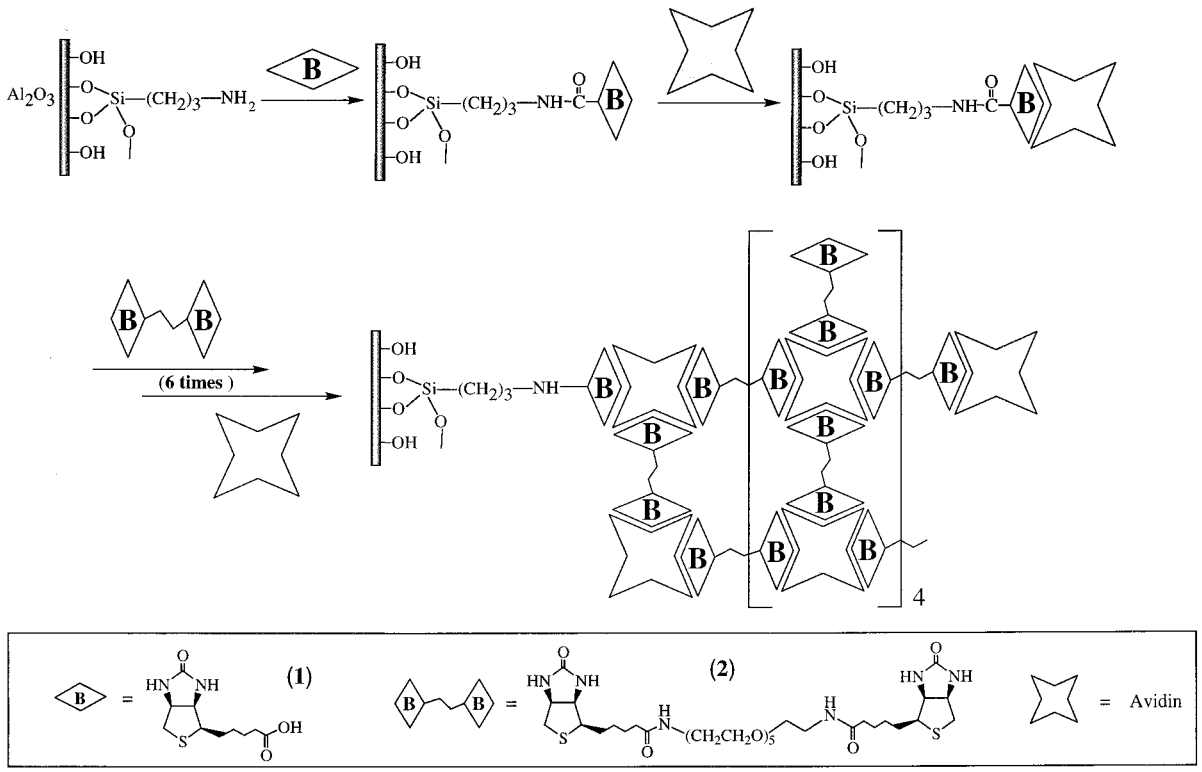

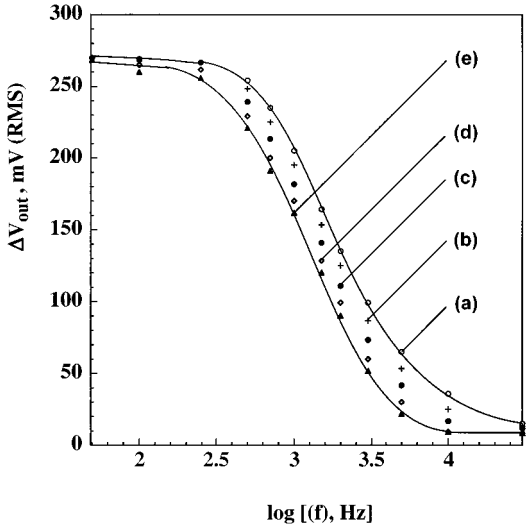

Figure 9. Output potentials of the ISFET device at different frequencies corresponding to (a) the DNP-antigen-functionalized gate interface; (b) after treatment with the DNP-Ab, 1.6×10^{-9} mg mL^{-1}; (c) after treatment with the DNP-Ab, 1.6×10^{-8} mg mL^{-1}; (d) after treatment with DNP-Ab, 1.6×10^{-7} mg mL^{-1}; (e) after treatment with DNP-Ab, 1.6×10^{-6} mg mL^{-1}.

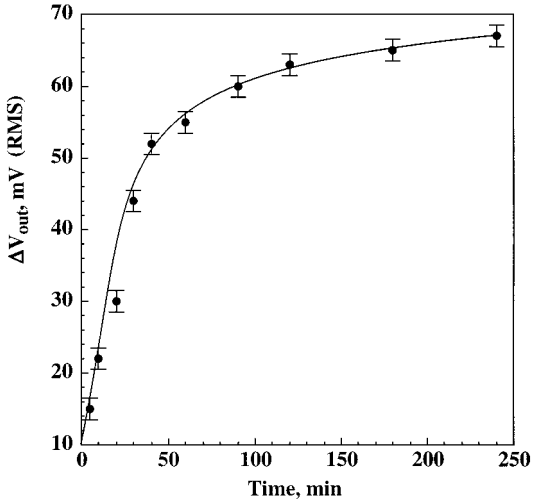

Figure 10. The change in the output potential, ΔV_{out}, as a function of time upon the interaction of the DNP-antigen-modified ISFET with the DNP-Ab, 1.6×10^{-6} M, for different time intervals. The ΔV_{out} are measured at 30 kHz.

and particularly, to determine the sensitivity limits of this method for the future development of immunosensors. Scheme 3 shows the method to functionalize the aminosiloxane layer, linked to the Al_2O_3 gate interface, with the dinitrophenyl antigen. *N*-2,4-Dinitrophenyl-ϵ-aminocaproic acid, (**3**), was covalently coupled to the siloxane layer. The association of the dinitrophenyl antibody, DNP-Ab, to the antigen layer was characterized by means of transconductance measurements as a means to analyze the antibody. Figure 9, curve (a), shows the ouput potential, ΔV_{out} of the DNP-antigen-functionalized gate interface, while Figure 9, curves (b) to (e), shows the output potential, ΔV_{out} curves after the interaction of the antigen-functionalized ISFET device with the DNP-Ab, $1.6 \times 10^{-9} - 1.6 \times 10^{-6}$ mg mL^{-1}, respectively, for 40 min. This bulk antibody concentration leads to the saturation of the antigen layer with the antibody (vide infra). As in the previous systems, the association of the DNP-Ab to the DNP-antigen interface results in a nonsymmetrical shift of the transconductance curve to low frequencies. Using eqs 5 and 6, the derived thickness of the DNP-Ab layer corresponds to 40 ± 5 Å. In contrast to glucose oxidase and avidin that exhibit a globular structure, the DNP-Ab exhibits a nonsymmetrical geometry with dimensions of ca. 50×70 Å. Realizing that the antibody has two-binding sites for the antigen and that the long Fc-axis of the antibody contributes mostly to the layer thickness, we expect that a random densely packed monolayer of the antibody would reveal an average thickness of ca. 42 Å, very close to the derived experimental value. It should be noted that in contrast to the biotin and GOx systems, that revealed a lower thickness for the respective first protein layer, the DNP-Ab system shows a protein layer thickness that is almost identical to the random densely packed assembly. This is attributed to the fact that the formation of antigen−antibody complexes requires precise spatial fitting. While GOx or avidin may associate to pores of the aminosiloxane film, thus leading to lower thickness values of the protein layers, the formation of the antigen−antibody complexes in the pores of the aminosiloxane film is sterically perturbed. As a result, the formation of the antigen−antibody complex occurs essentially on the surface of the aminosiloxane film, leading to overlapping values of the film thickness and the antibody dimensions.

The fact that the frequency-dependent transconductance measurements enable us to probe the association of the antibody to the antigen-functionalized interface, suggests that we could apply the method as an electronic transduction means to follow the formation of antigen−antibody complexes on the gate surface of the ISFET device. Thus, one may use this approach to develop immunosensors.

Figure 10 shows the response of the antigen-functionalized ISFET device upon interaction with the DNP-Ab, 1.6×10^{-6}

SCHEME 3: Functionalization of the ISFET Device with the Antigen (3) and the Formation of the Antigen/DNP-Ab Complex on the Gate Interface

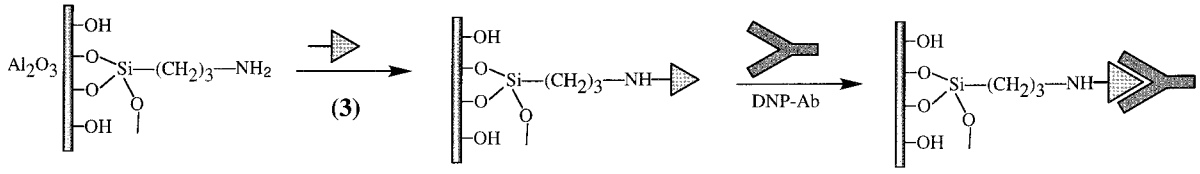

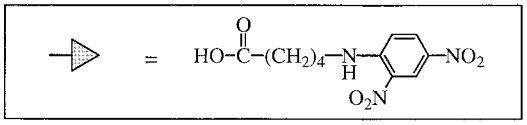

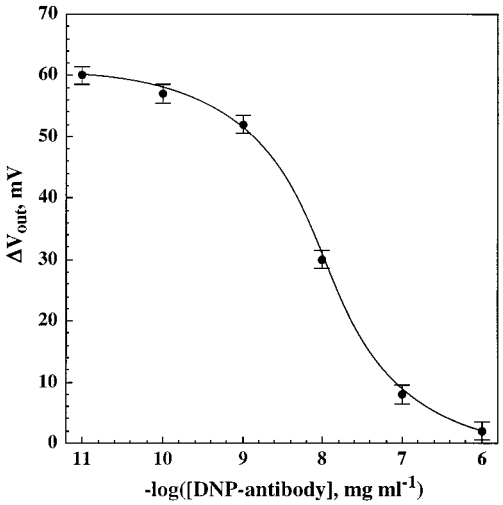

Figure 11. Response of the DNP-antigen-functionalized ISFET to various concentrations of the DNP-Ab for a fixed time-interval of 40 min recorded at 30 kHz.

mg mL^{-1}, for various time intervals. In this experiment, the output potential ΔV_{out} is measured at a constant frequency of 30 kHz, and the difference between the V_{out} of the antigen-functionalized ISFET and the V_{out} of the antigen/DNP-Ab-functionalized ISFET is recorded. It can be seen that in the first 40 min of the interaction of the antigen-functionalized ISFET with the DNP-Ab, the most significant changes in ΔV_{out} are observed. Thus, the sensing of variable concentrations of the DNP-Ab was performed by the interaction of the antigen-modified ISFET with the antibody for a fixed time interval that corresponds to 40 min.

Figure 11 shows the ΔV_{out} values observed upon the sensing of variable concentrations of the DNP-Ab. The output potential curves are shown in Figure 9. The ΔV_{out} values shown in Figure 11 are extracted from these curves at a frequency of 30 kHz, where the highest difference in the ΔV_{out} values is observed. It is evident that the antigen-functionalized ISFET device, and the respective electronic transduction method, enable us to sense the DNP-Ab in the concentration range that corresponds to 0.1 ng mL^{-1} to 1 μg mL^{-1}. The linear response range of the device is in the concentration range of 1 ng mL^{-1} to 100 ng mL^{-1} with a slope that corresponds to 22 mV dec^{-1}. The lower detection limit of the sensor for the analysis of the DNP-Ab is 0.6 ng mL^{-1}. The upper detection limit of the DNP-Ab by the ISFET sensor is 250 ng mL^{-1}, and at higher concentrations, the gate surface is saturated by the DNP-Ab.

Conclusions

Our study has presented a novel method that is based on impedance measurements to characterize protein architectures assembled on the gate interface of an ISFET device. To date, the structural characterization of ISFET gate interfaces modified with biomaterials or polymer films was almost impossible, leading to difficulties in the reproducible production of the sensing interfaces. In the present study we were able to characterize the thickness of layered protein assemblies on the gate interface by impedance. Knowing the structural features of the proteins, and the respective layer thickness, the surface coverage per layer of the respective proteins could be estimated. To apply the impedance spectroscopy as a generic methodology to characterize layered protein nanostructures on the gate interface of ISFET devices, one important prerequisite must be fulfilled. That is, the protein layer(s) should exhibit a substantially lower thickness as compared to the thickness of the oxide-layer or membrane associated with the gate surface. Using the impedance spectroscopy method, we were able to characterize layered assemblies consisting of glucose oxidase and of biotin-cross-linked avidin. Similarly, the method was applied to characterize the formation of antigen−antibody complexes on the gate surface.

The ability to characterize the structures of protein layers on the gate surface by ISFET devices by means of impedance spectroscopy not only provides a method for the structural characterization of the systems, but also yields an analytical method to probe and sense biorecognition events that occur on the gate surface of the ISFET. We believe that impedance spectroscopy could provide a versatile method to characterize other functionalized ISFET systems, i.e., modified with neurons, cells, or DNA. Similarly, the method could be further advanced by its application for the amplified sensing of antigen−antibody interactions by the use of anti-antibodies, and by the probing of protein−protein and DNA−protein interactions.

Acknowledgment. This research is supported by The Israel Ministry of Science as an infrastructure project in biomicro-electronics.

References and Notes

(1) (a) Izquierdo, A.; de Castro, M. D. L. *Electroanalysis* **1995**, *7*, 505. (b) Scheller, F. W.; Schubert, F.; Neumann, B.; Pfeiffer, D.; Hintsche, R.; Dransfeld, I.; Wollenberger, U.; Renneberg, R.; Warsinke, A.; Johansson, G.; Skoog, M.; Yang, X.; Bogdanovskaya, V.; Zaitsev, S. Y. *Biosens. Bioelectron.* **1991**, *6*, 245.

(2) (a) Schroth, P.; Schöning, M. J.; Schütz, S.; Malkoc, Ü.; Steffen, A.; Marso, M.; Hummel, H. E.; Kordos, P.; Lüth, H. *Electrochim. Acta* **1999**, *44*, 3821. (b) Shiono, S.; Hanazato, Y.; Nakako, M. *Method Biochem. Anal.* **1992**, *36*, 151. (c) Bergveld, P.; Sibbald, A. *Analytical and Biomedical Applications of ISFETs*; Elsevier: Amsterdam, 1988.

(3) (a) Senillou, A.; Jaffrezic-Renault, N.; Martelet, C.; Cosnier, S. *Talanta* **1999**, *50*, 219. (b) Vianello, F.; Stefani, A.; Di Paolo, M. L.; Rigo, A.; Lui, A.; Margesin, B.; Zen, M.; Scarpa, M.; Soncini, G. *Sens. Actuators B* **1996**, *37*, 49. (c) Vering, T.; Schuhmann, W.; Schmidt, H.-L.; Mikolajick, T.; Falter, T.; Ryssel, H.; Janata, J. *Electroanalysis* **1994**, *6*, 953. (d) Sevilla, F. III.; Kullick, T.; Scheper, T. *Biosens. Bioelectron.* **1994**, *9*, 275. (e) Reshetilov, A. N.; Donova, M. V.; Dovbnya, D. V.; Boronin, A. M.; Leathers, T. D.; Greene, R. V. *Biosens. Bioelectron.* **1996**, *11*, 401.

(4) (a) Volotovsky, V.; Kim, N. *Electroanalysis* **1998**, *10*, 512. (b) Hendji, A. M. N.; Jaffrezic-Renault, N.; Martelet, C.; Clechet, P.; Shul'ga, A. A.; Strikha, V. I.; Netchiporuk, L. I.; Soldatkin, A. P.; Wlodarski, W. B. *Anal. Chim. Acta* **1993**, *281*, 3. (c) Pijanowska, D. G.; Torbicz, W. *Sens. Actuators B* **1997**, *44*, 370. (d) Volotovsky, V.; Soldatkin, A. P.; Shul'ga, A. A.; Rossokhaty, V. K.; Strikha, V. I.; El'skaya, A. V. *Anal. Chim. Acta* **1996**, *322*, 77. (e) Dzyadevich, S. V.; Korpan, Y. I.; Arkhipova, V. N.; Alesina, M. Y.; Martelet, C.; El'skaya, A. V.; Soldatkin, A. P. *Biosens. Bioelectron.* **1999**, *14*, 283.

(5) (a) Sekiguchi, T.; Nakamura, M.; Kato, M.; Nishikawa, K.; Hokari, K.; Sugiyama, T.; Asaka, M. *Sens. Actuators B* **2000**, *67*, 265. (b) Koncki, R.; Owczarek, A.; Dzwolak, W.; Glab, S. *Sens. Actuators B* **1998**, *47*, 246.

(6) Kharitonov, A. B.; Zayats, M.; Lichtenstein, A.; Katz, E.; Willner, I. *Sens. Actuators B* **2000**, *70*, 222.

(7) Zayats, M.; Kharitonov, A. B.; Katz, E.; Bückmann, A. F.; Willner, I., *Biosens. Bioelectron.* **2000**, *15*, 671.

(8) Willner, I.; Katz, E. *Angew. Chem., Int. Ed.* **2000**, *39*, 1180.

(9) Willner, I.; Katz, E.; Willner, B. *Electroanalysis* **1997**, *13*, 965.

(10) Antonisse, M. M. G.; Snellink-Ruël, B. H. M.; Lugtenberg, R. J. W.; Engbersen, J. F. J.; van den Berg, A.; Reinhoudt, D. N. *Anal. Chem.* **2000**, *72*, 343.

(11) Druise, J.; Ripens, J. G.; Bergveld, P.; Kremer, F. J. B.; Starmans, J. R.; Maak, J.; Feijen, J.; Reinhoudt, D. N. *Sens. Actuators B* **1992**, *6*, 101.

(12) Lugtenberg, R. J. W.; Egberink, R. J. M.; van den Berg, A.; Engbersen, J. F. J.; Reinhoudt, D. N. *J. Electroanal. Chem.* **1998**, *452*, 69.

(13) Souteyrand, E.; Cloarec, J. P.; Martin, J. R.; Wilson, C.; Lawrence, I.; Mikkelsen, S.; Lawrence, M. F. *J. Phys. Chem. B* **1997**, *101*, 2980.

(14) Prasard, B.; Lal, R. *Meas. Sci. Technol.* **1999**, *10*, 1097.
(15) Chovelon, J. M.; Jaffrezic-Renault, N.; Gros, Y.; Fombon, J. J.; Pedone, D. *Sens. Actuators B* **1991**, *3*, 43.
(16) Bousse, L.; Bergveld, P. *J. Electroanal. Chem.* **1983**, *152*, 25.
(17) Maupas, H.; Saby, C.; Martelet, C.; Jaffrezic-Renault, N.; Soldatkin, A. P.; Charles, M. H.; Delair, T.; Mandrand, B. *J. Electroanal. Chem.* **1996**, *406*, 53.
(18) Schyberg, C.; Plossu, C.; Barbier, D.; Jaffrezic-Renault, N.; Martelet, C.; Maupas, H.; Souteyrand, E.; Charles, M. H.; Delair, T.; Mandrand, B. *Sens. Actuators B* **1995**, *27*, 457.
(19) Friebe, A.; Lisdat, F.; Moritz, W. *Sens. Mater.* **1993**, *5*, 65.
(20) Armstrong, R. D.; Horvai, G. *Electrochim. Acta* **1990**, *35*, 1.
(21) Bergveld, P.; van den Berg, A.; van der Waal, P. D.; Skowronska-Ptasinska, M.; Sudhölter, E. J. R.; Reinhoudt, D. N. *Sens. Actuators B* **1989**, *18*, 309.
(22) Demoz, A.; Verpoorte, E. M. J.; Harrison, D. J. *J. Electroanal. Chem.* **1995**, *389*, 71.
(23) Lion-Dagan, M.; Marx-Tibbon, S.; Katz, E.; Willner, I. *Angew. Chem., Int. Ed. Engl.* **1995**, *34*, 1604.
(24) http://www.rcsb.org/pdb.
(25) Garrett, R. H.; Grisham, C. M. *Biochemistry*; Saunders College Publishing: Fort Worth, 1995; p 495.